The dark clouds of being a social outcast

Asscheman, J.S.

2020

document version
Publisher's PDF, also known as Version of record

Chapter 4

Associations between Peer Attachment and Neural Correlates of Risk Processing Across Adolescence

Published as:
Asscheman, J.S., Deater-Deckard, K., Lauharatanahirun, N., van Lier, P.A.C., Koot, S., King-Casas, B., & Kim-Spoon, J. (2020). Associations between peer attachment and neural correlates of risk processing across adolescence. *Developmental Cognitive Neuroscience, 42*, 100772.

Abstract

Adolescence is a period of increased risk-taking behavior where individual differences in risk taking may relate to both adverse and positive experiences with peers. Yet, knowledge on how risk processing develops in the adolescent brain and whether this development is related to peer attachment is limited. In this longitudinal functional magnetic resonance imaging (fMRI) study, we collected data from 167 adolescents (53% male) followed for four annual assessments across ages 13 – 17 years. At each assessment, participants completed a lottery choice task to assess neural risk processing and reported on their perceived attachment to peers and parents. Behaviorally, risk-preference on the lottery choice task decreased linearly with age. Neural activation during risk processing was consistently found in the insula and dACC across the four assessments and increased linearly from ages 13 – 17 years. Furthermore, higher peer attachment was related to greater right insula risk processing for males but not for females, even after controlling for parental attachment. The magnitudes of this association did not change with age. Findings demonstrate that neural risk processing shows maturation across adolescence and high peer attachment may be associated with low risk taking by heightening neural sensitivity to potential risks for male adolescents.

Introduction

Adolescence is characterized by increased risk-taking behavior that is considered, in part, to be normative explorative behavior important for adolescents' social and emotional development (Collado, Felton, MacPherson, & Lejuez, 2014; Crone, van Duijvenvoorde, & Peper, 2016). However, some adolescents engage in high levels of risky behaviors (e.g., smoking, drug use, reckless driving) which may have serious health consequences (Kann et al., 2018). Increased risk-taking behavior has been related to adverse peer experiences (e.g., social exclusion) and such experiences may be linked to the development of neural circuitries implicated in risk processing (Burnett, Sebastian, Kadosh, & Blakemore, 2011; Foulkes & Blakemore, 2018; Schriber & Guyer, 2016). Yet, our understanding of the development of risk processing in the adolescent brain and whether this neural risk processing is associated with positive peer experiences, such as peer attachment, is still limited.

Risk-taking behavior during adolescence is driven by the recruitment of several brain regions including the insula, dorsomedial prefrontal cortex (dmPFC)/dorsal anterior cingulate cortex (dACC), ventral striatum, orbitofrontal cortex, and lateral prefrontal cortex (Platt & Huettel, 2008; Sherman, Steinberg, & Chein, 2018). These brain regions may contribute to risk-taking behavior through two different processes. That is, increased risk-taking behavior during adolescence is thought to arise from a neural imbalance between a hyper-responsive socio-emotional system and a more slowly developing cognitive control system (Casey, Jones, & Hare, 2008; Steinberg, 2007). Prior studies have focused mainly on increased neural responsivity to rewards during risk taking (Silverman, Jedd, & Luciana, 2015; van Duijvenvoorde, Peters, Braams, & Crone, 2016), but another important process that may guide risk-taking behavior is the neural evaluation of risks (d'Acremont & Bossaerts, 2008; van Duijvenvoorde et al., 2015). However, research is still limited on the neural development of the latter process during adolescence.

Two regions that may be especially important for risk processing and guiding adolescent risk behavior are the insula and dACC. Extant literature in adults and adolescents implicates the insular cortex and dACC in risk processing (see meta-analysis by Mohr, Biele, & Heekeren, 2010; Platt & Huettel, 2008; Schonberg, Fox, & Poldrack, 2011). Longitudinal studies on the development of risk processing in the insula and dACC are lacking. Some cross-sectional neuroimaging studies found that, during risky decisions (e.g., choosing risky options over safe options), adults showed higher insula and dACC activation compared to adolescents and children (Paulsen, Carter, Platt, Huettel, & Brannon, 2012). In contrast, other cross-sectional neuroimaging studies found an age-related decrease in medial PFC/dACC activation for high-risk choices (compared to low-risk choices) among children, adolescents,

and adults (van Leijenhorst, Crone, & Bunge, 2006; van Leijenhorst et al., 2010). Finally, one study examining neural sensitivity to risk information (i.e., outcome variability) found that insula and dmPFC/ dACC activation were hyperactive in adolescents compared to children and adults, and that higher activation in the insula and dmPFC/dACC was related to greater risk-averse behavior among adolescents (van Duijvenvoorde et al., 2015). These results suggest the importance of the insula and dACC for guiding risk-related decision making particularly among adolescents.

However, because of the cross-sectional nature, prior studies did not assess within-person changes in risk-related neural processing and were limited in making developmental inferences. The mixed findings reported in the current literature may be in part due to of the fact that prior cross-sectional studies compared different age groups: different studies had different age ranges to represent children, adolescent, and adult groups, and only small numbers of individuals were included in each age group (i.e., 12 to 25 people per age group). In the current study, we examined the development of neural risk processing by studying within-person changes in the insula and dACC across adolescence using a relatively large sample size of adolescents who were assessed repeatedly from 13 to 17 years.

Besides increased risk-taking behavior, adolescence is also characterized by an increased sensitivity to the peer environment (Nelson, Leibenluft, McClure, & Pine, 2005). As such, the peer environment may contribute to the development of risk-taking behavior and associated neural circuitries (Burnett et al., 2011; Schriber & Guyer, 2016). For example, prior studies showed that the presence of peers and winning a risky gamble for friends were linked to increased activation in brain regions related to reward processing (i.e., striatum activation) during risk taking (Braams, Peters, Peper, Güroğlu, & Crone, 2014; Chein, Albert, O'Brien, Uckert, & Steinberg, 2011; Powers et al., 2018). Also, the quality of peer relationships, such as the level of attachment to peers, has been shown to be positively related to adolescent risk-taking behaviors (Piko, 2000; Urberg, Luo, Pilgrim, & Degirmencioglu, 2003; Wills, Resko, Ainette, & Mendoza, 2004) and to be linked to increased activation in brain regions associated with the socio-emotional system (e.g., medial prefrontal cortex) during risk taking (Telzer, Fuligni, Lieberman, Miernicki, & Galvan, 2015). Research also found an association between high friendship quality and increased activation in the striatum when winning a gamble for friends, but only for female adolescents (Braams et al., 2014) but this association between high friendship quality and increased activation in the striatum was not found consistently (Braams & Crone, 2016, 2017).

Thus, studies indicate a link between the peer environment and heightened neural activation related to *reward*. It is unknown, however, whether positive peer experiences such as peer attachment may be associated with adolescents' neural

sensitivity to *risk*. Prior studies suggest two opposing effects that peer attachment may have on neural risk processing. On the one hand, a prior study found that high levels of peer attachment may protect adolescents from risky behavior (Telzer et al., 2015). Accordingly, high levels of peer attachment may heighten adolescents' sensitivity to risk information, ultimately resulting in low risk-taking behaviors. On the other hand, high levels of peer attachment may increase risk-seeking tendencies because peers may heighten the positive affect among adolescents. Adolescents high in peer attachment might experience higher positive affect from peers, compared to adolescents low in peer attachment, which may decrease the perceived riskiness of decisions (Romer & Hennessy, 2007). Furthermore, adolescents with high peer attachment may engage in greater peer socialization of risky behavior via social learning, compared to their counterparts with low peer attachment (Brechwald & Prinstein, 2011; Jessor, 1993; Kandel, 1985). As a result, higher peer attachment may be associated with lower neural sensitivity to risk information. It is difficult to ascertain which effect is more likely because the nature of the tasks used in prior studies examining peer influences on adolescent brain functioning were not able to separate risk processing from reward processing. Moreover, prior studies were limited in their ability to evaluate developmental changes in peer influences on neural processing due to the cross-sectional nature of their fMRI data.

When studying the association between peer attachment and neural risk processing during adolescence, potential sex differences also need to be considered. To our knowledge, no prior study has examined sex differences in the associations between peer attachment and neural processing of risk information. However, one prior study found a positive association between friendship quality and neural reward processing during risk choices involving friends for females only (Braams et al., 2014). Moreover, sex differences in peer attachment experiences are known to exist. Females value relationship intimacy more, seek more support from peers, and disclose more information to their peers than males (Gorrese & Ruggieri, 2012; Rose & Rudolph, 2006). These sex differences may result in differences in how adolescents' peer attachment is associated with the processing of risk information in their brains. Given the lack of prior empirical studies, we explored adolescent sex as a statistical moderator in the present study.

The current study had two main goals. First, we examined the development of neural risk processing and tested potential sex differences across adolescence, from ages 13 – 17 years. We focused on the insula and dACC based on extensive literature implicating these regions in risk processing. We hypothesized that risk processing activity in the insula and dACC would increase with age, based on previous cross-sectional studies showing both higher activation during risk processing in adults compared to adolescents and children (Eshel, Nelson, Blair, Pine, & Ernst, 2007;

Paulsen et al., 2012) and a suggested increase in risk-related activation in these regions among adolescents compared to children (van Duijvenvoorde et al., 2015). In addition, we were interested in knowing whether risk processing is specific to the insula and dACC, or if it involves other brain regions that have been shown to activate during risk-taking behavior such as the ventral striatum, orbitofrontal cortex, and lateral prefrontal cortex. Second, we further examined whether the development of neural risk processing was associated with peer attachment. Specifically, using longitudinal data spanning ages 13 – 17 years, we examined how peer attachment is associated with the development of neural processing of risk evaluation which was assessed using an economic risky decision-making task. In doing so, we additionally tested for sex differences in the association between neural risk processing and peer attachment.

Method

Participants

The sample consisted of 167 adolescents (53% males) from rural-to-urban areas in an Appalachian region of southwestern Virginia in the United States of America. Data were collected on four annual assessments in 2014 (T1; *M*age = 14.13 years, *SD* = 0.54), 2015 (T2; *M*age = 15.05 years, *SD* = 0.54), 2016 (T3; *M*age = 16.08 years, *SD* = 0.55), and 2017 (T4, *M*age =17.01 years, *SD* = 0.55). At T1, data from 157 adolescents were collected. Seventeen adolescents did not return at T2 due to lost contact, declined participation or ineligibility for the task (i.e., brain abnormality, not meeting MRI safety criteria). Therefore, at T2 10 additional participants were included to reach a sample size of 167 adolescents. At T3 data from 147 participants, and at T4 data from 150 participants were collected. Participants who did not participate in one annual assessment were still invited to participate in the following assessments. Overall, 24 adolescents did not participate at all possible time points for reasons including: ineligibility for tasks (n = 2), declined participation (n = 17), and lost contact (n = 5) during the follow-up assessments. Attrition analyses using general linear model (GLM) univariate procedures indicated that the rate of participation (indexed by proportion of years participated to years invited to participate) was not significantly predicted by demographic variables (p = .61 for age, p = .67 for income, p = .62 for sex, and p = .73 for race, contrasted as White vs non-White).

Adolescents were identified as 82% Caucasian, 12% African-American, and 6% other. The mean of the annual family household income fell between $25,000 and $34,999 at T1, which is below the median household income ($57,652) of the United States of America during the study period spanning the mid-2010s (Census, 2017).

Ethnicity and household income of the current sample were representative for the area in which data were collected.

Procedure

Participants were recruited through advertisement using flyers, letters, and emails. Adolescents with MRI contraindications (e.g., dental braces, history of head injuries) were excluded from participation. During each annual assessment, adolescents participated in a five-hour session at the university which was supervised by a trained research assistant. Participants filled out questionnaires and completed a two-hour MRI session in which an anatomical scan was acquired followed by several fMRI tasks of which the risk-taking task was the first. Parents were informed about the study and provided written informed consent while adolescents provided written assent. Adolescents were monetarily compensated at the end of each annual visit for their participation. All study procedures were approved by the Institutional Review Board of Virginia Tech.

Measures

Peer attachment. Adolescents reported annually on their perceived attachment to peers and parents using a shortened version of the Inventory of Parent and Peer Attachment (IPPA; Armsden & Greenberg, 1987; Raja, McGee, & Stanton, 1992). The IPPA is designed to assess adolescents' perceptions of the quality of psychological security provided by parents and peers as well as how accessible and responsive these attachment figures are. The shortened version consisted of 12 items on three subscales (4 items per scale): trust, communication, and alienation. The trust subscale assessed the degree of mutual trust parents and peers provide (e.g., "*I can count on my friends when I need to get something off my chest.*"). The communication subscale assessed the perceived quality of communication between adolescents and their parents or peers (e.g., "*When we discuss things, my friends care about my point of view*"). The alienation subscale assessed the extent of anger or alienation adolescents experience in their relationship with parents or peers (e.g., "*Talking over my problems with friends makes me feel ashamed or foolish*"). Items could be answered on a five-point Likert scale ranging from Never or Almost Never (1) to Always or Almost Always (5). Negative items were reverse coded and a mean score of the 12 items regarding peer attachment was computed such that higher scores indicated higher perceived peer attachment. Cronbach's alphas ranged between .78 – .84 over the four assessments. The IPPA has been shown to have good reliability and validity to assess the quality of the attachment to parents and peers (Gullone & Robinson, 2005; Jewell et al., 2019).

Lottery choice task. The current study adopted a behavioral economic definition of risk, which is defined as the variance between potential outcomes and which allows for the decomposition of risk in a risk and return component (Schonberg et al., 2011). At each yearly assessment, adolescents completed a modified economic lottery choice task (Holt & Laury, 2002) while their blood-oxygen-level dependent (BOLD) responses were recorded. On each trial, participants could choose between two uncertain gambles. Both gambles consisted of a low and a high outcome option, and probabilities for the low and high outcome were the same in both gambles. However, one gamble was riskier because there was a large difference between the high and low outcome (e.g., $3.85 vs $0.10), while the safer gamble had a small difference between the high and low outcome (e.g., $2.00 vs $1.60). Choosing the riskier option would mean a chance of receiving a larger reward at the risk of receiving a much smaller reward, whereas choosing for the safer option would mean that the reward would be similar regardless. The simultaneous presentation of the two gambles was intended to simulate real-world decision options in which individuals are often faced with more than one option, in which some choices are riskier than others.

Participants completed a total of 72 trials in about 25 minutes. Trials started with a decision phase in which one pair of gambles (a risky and safer option) was presented for four seconds (see Figure 4.1). Probabilities and the associated outcomes for these probabilities were presented in purple and orange. Probabilities of each outcome were presented as slices of a pie to increase the numerical understanding of the gamble. The pie consisted of 10 slices with each slice representing 10% probability. Probabilities of the outcomes were the same for each pair of gamble options and were randomly varied across trials (see Supplementary Table S4.1). Participants could indicate their choice of gamble with a press on a fMRI compatible button box using their left or right hand, which was randomized across participants. After the decision phase a fixation cross was presented with a jitter of 1 – 3 seconds. Following the fixation period, an outcome screen showed the outcome of the chosen gamble for two seconds. A jittered intertrial interval (ITI) of 1 – 3 seconds was presented before the start of the next trial. Participants completed six practice trials prior to the fMRI task. Participants received their outcome on four random trials as an additional monetary reward for their participation. Participants were instructed that each trial was independent of the other trial and evenly likely to be selected for payment.

As a behavioral indicator of risk taking we computed a risk-preference parameter for each participant using a standard utility power function with higher values indicating higher risk-seeking behavior (see Supplementary material: Risk-preference parameter). Prior studies used the lottery choice task with adolescents and showed

that neural responses during this task predicted real-life risky behaviors (Kim-Spoon et al., 2019; Kim-Spoon et al., 2017, 2019).

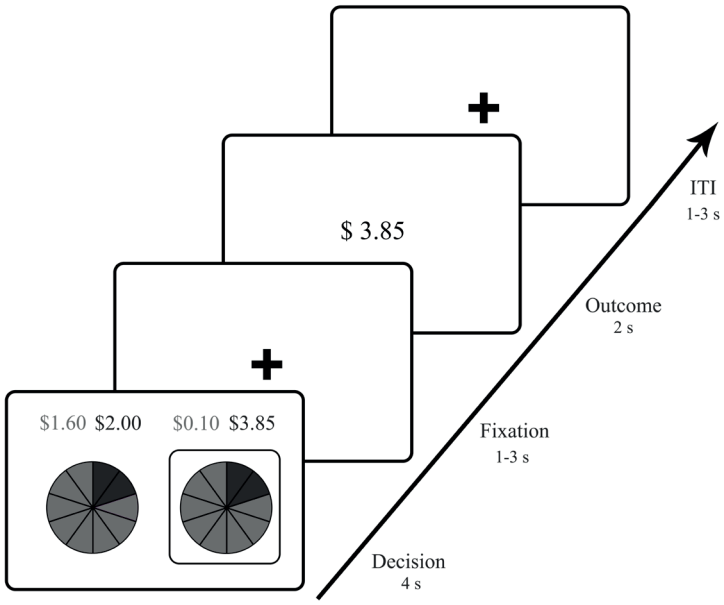

Figure 4.1. Lottery choice task. On each trial, two gambles were presented with the same probabilities of winning a high or low outcome. However, gambles differed on the variance in low and high outcome. That is, on riskier gambles (right gamble) the difference between the high and low outcome was larger ($3.85 - $0.10) than on the safer gambles (left gamble, $2.00 - $1.60). Outcomes and probabilities were presented in corresponding colors (purple and orange). The decision phase was followed by a fixation screen after which the outcome on the chosen gamble was shown. Trials ended with a jittered inter-trial interval (ITI).

Control variables

Parental attachment. Prior studies indicated that parental attachment is associated with risk-taking behavior and associated neural responses (Qu, Fuligni, Galvan, & Telzer, 2015). Therefore, to examine the unique effects of peer attachment on neural risk processing, rather than the individual's general tendency of being attached to people, parental attachment was added to our mixed models (see method section 2.7.1). Parental attachment was assessed using the IPPA (see measures section 2.3.1). Adolescents answered the same 12 attachment items for maternal and paternal attachment separately. Negative items were reverse coded and a mean score was computed for maternal and paternal attachment. To create one measure of parental attachment we used the highest score for either maternal or paternal attachment as an index for perceived parental attachment. Cronbach's

alphas ranged between .74 – .83 over the four assessments. Similar to other studies, we found that the correlations between peer and parent attachments were low to moderate, ranging between *r* = .04 and .34 (see Supplementary Table S4.2; Armsden & Greenberg, 1987; Raja et al., 1992).

Pubertal development. Prior studies showed that pubertal development is associated with activation in reward-related regions during risk taking (Goddings, Beltz, Peper, Crone, & Braams, 2019). Therefore, pubertal development was included in our mixed models (see method section 2.7.1) to investigate neural changes across adolescence over and above the effects that can be explained by pubertal development. Physical pubertal development was assessed using the adolescent self-rating scale of the Pubertal Developmental Scale (Petersen, Crockett, Richards, & Boxer, 1988). The questionnaire consisted of five items that assessed physical pubertal development such as growth spurts, body hair changes, and skin changes. In addition, female adolescents were asked to report on their breast development and menarche, and male adolescents were asked to report on vocal changes and facial hair changes. Items could be answered using a four-point Likert scale, ranging from 1 (no changes) to 4 (changes completed). A mean score of the items was computed as an index for pubertal development. Higher scores indicated more advanced pubertal development. Cronbach's alphas ranged between .44 - .55 over the four assessments. Correlations between pubertal development and age were relatively low, ranging between *r* = -.01 and .22.

Imaging acquisition

Scans were acquired using a 3.0 Tesla Siemens Tim Trio scanner and a 12-channel head coil (Siemens Healthcare, Erlangen, Germany). Participants could view the screen through a mirror mounted on the head coil. Whole-brain echo-planar imaging (EPI) was used to acquire functional images during the lottery choice task (repetition time (TR) = 2000 ms, echo time (TE) = 30 ms, field of view (FOV) = 220 x 220 mm, 64 x 64 grid, voxel size = 3.4 x 3.4 x 3.4 mm, flip angle = 90 °, 34 axial slices, and 4.0 mm slice thickness). Hyperangulated slices were acquired at 30 degrees from anterior-posterior commissure. For within-subject registration, a whole-brain T1-weighted anatomical scan was acquired using high-resolution magnetization prepared rapid acquisition gradient echo sequence (192 slices, TR = 1200 ms, TE =2.66 ms, FOV = 245 x 245 mm, voxel size = 1 x 1 x 1 mm). There were 141 valid scans obtained at T1, 136 at T2, 126 at T3, and 129 at T4 (see Supplementary Table S4.3). Reasons for excluding scans include not meeting MRI safety criteria, excessive head motion (>3 mm), technical errors, or imaging artifacts.

fMRI preprocessing and analysis

Functional images were preprocessed and analyzed using Statistical Parametric Mapping version 8 (SPM8: Wellcome Centre for Human Neuroimaging, London, UK). Functional images were realigned using six rigid body transformation parameters. To correct for the timing differences in slice acquisition, slice time correction was performed. The mean functional image was co-registered with the anatomical image. The T1-weighted anatomical image was segmented and co-registered to the Montreal Neurological Institute template using the unified segmentation approach with a resampling rate of 3 x 3 x 3 mm voxel size (Ashburner & Friston, 2005). These co-registration parameters were used to normalize the functional images. Finally, normalized images were smoothed with a Full Width Half Maximum Gaussian kernel of 6 mm.

For each yearly assessment, a first-level general linear model (GLM) was conducted which included one regressor for the decision period and one regressor for the outcome period with a fixed duration of four and two seconds, respectively. A parametric regressor was included that coded for the magnitude of risk of a chosen gamble on each trial to examine which brain regions were sensitive to the magnitude of risk. To this end, we quantified the amount of risk associated with each gamble during the lottery choice task by computing the coefficient of variation (CV; see Supplementary material). The CV is a scale-free metric and has been shown to be superior in explaining choice behavior compared to other economic measures of risk (i.e., standard deviation or variance) because outcomes are coded by the relative risk as opposed to the absolute outcome (Bach, Symmonds, Barnes, & Dolan, 2017; Weber, Shafir, & Blais, 2004). The CV is computed by dividing the standard deviation of the chosen gamble by the expected value (i.e., probability-weighted outcome) of that gamble, with higher levels of CV corresponding to a higher variance between the high and low outcome on a gamble and thus higher risk (see Supplementary Table S4.1). The CV of the chosen gamble on each trial was added as a parametric regressor to the GLM. Another parametric regressor was added to the GLM that coded for high and low outcomes during the outcome phase to assess outcome processing. Furthermore, one regressor for the button press and six motion regressors were included. These regressors of interest and no interest were included to appropriately characterize the error term in the neural model. Regressors were convolved with a canonical hemodynamic response function. Data were prewhitened to remove temporal autocorrelation (AR1) and high-pass filtered at 128 Hz.

First-level images from each year assessing neural responses associated with the CV of the chosen gamble during the decision were submitted to whole-brain random-effect analysis separately. On each assessment, the CV of the chosen

gamble was significantly associated with the BOLD responses in the insula and dACC, such that choosing riskier gambles was related to higher BOLD responses in the insula and dACC (Figure 4.2).

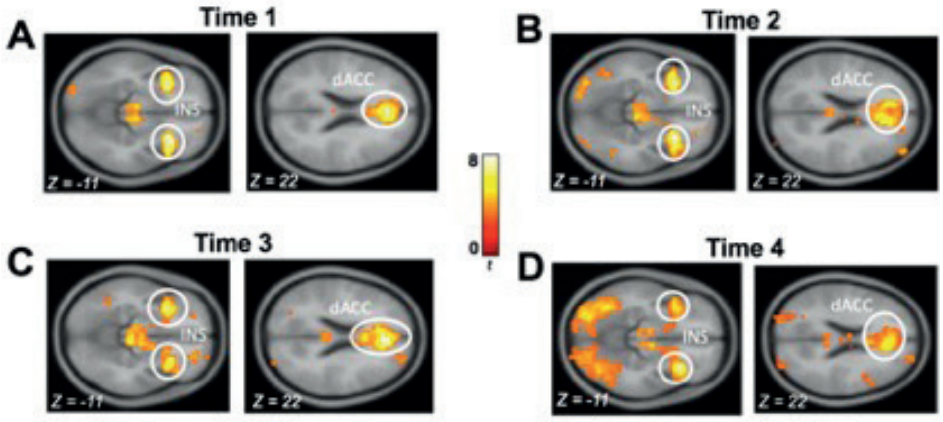

Figure 4.2. During the decision phase increased activation was found in the insula (INS) and dorsal anterior cingulate cortex (dACC) during riskier gambles as was indicated by the coefficient of variation (CV).

All statistical inferences were made at a cluster-corrected threshold of $p < .05$ with a Family-Wise Error (FWE) correction, with an initial uncorrected threshold of $p < .001$. Results indicated that the bilateral insula and dACC belonged to the largest regions, with the greatest *t*-values, among the regions activated in response to the differing levels of risk in our task (see Supplementary Tables S4.4-S4.7). Additionally, they were the most consistently activated brain regions across all four waves in our longitudinal assessments. In contrast, activation in the ventral striatum, orbitofrontal cortex, and lateral prefrontal cortex was not consistent across assessments. This is not surprising given the large body of literature in both adolescents (e.g., van Duijvenvoorde et al., 2015) and adults (e.g., Mohr et al., 2010) indicating that the insula and dACC are key regions consistently reported to represent economic risk in the brain. Accordingly, only the bilateral insula and dACC were considered in the main analyses. For consistent comparison of each yearly assessment, eigenvariate values from the bilateral insula and the dACC were extracted using a standard neuroanatomical atlas for functional neuroimaging data (Automated Anatomical Labeling (AAL) (Tzourio-Mazoyer et al., 2002) using SPM (see Supplementary Figure S4.1). Once the anatomical ROIs were extracted, we performed our statistical analyses.

Statistical analyses

Mixed model building procedure. We used a mixed model approach in R (R core Team, 2018) using the nlme package (Pinheiro, Bates, DebRoy, & Sarkar, 2018). Mixed models are appropriate for nested data such as longitudinal data as they allow for the estimation of average starting points and trajectories in the sample (i.e., fixed intercepts and slopes) while at the same time allowing for individual variation in starting points and trajectories over time (i.e., random intercepts and slopes). Data were missing completely at random (Little MCAR test: χ^2 = 586.11, *df* = 666, *p* = .981) and therefore multiple imputation was used with the MICE package in R (van Buuren & Groothuis-Oudshoorn, 2011). Missing data on neural risk processing, peer attachment and covariates were imputed. Imputing data that are missing completely at random has been shown to not bias parameter estimates (Ambler, Omar, & Royston, 2007; Donders, van der Heijden, Stijnen, & Moons, 2006; Little, 1992; Rubright, Nandakumar, & Glutting, 2014). Moreover, multiple imputations have been shown to outperform deletion methods (Enders, Mistler, & Keller, 2016; Newman, 2003).

Our first goal was to assess the development of neural risk processing in the insula and dACC across adolescence using a formal fitting approach (Braams & Crone, 2017; Braams, van Duijvenvoorde, Peper, & Crone, 2015). Neural risk processing in the insula and dACC were fitted separately using a maximum likelihood estimation (for the full model see Supplementary material). First, a null model that included both a fixed and random intercept was fitted. Next, we compared the null model against a set of models assessing developmental changes (i.e., linear, quadratic, cubic) by adding age (mean-centered) as a polynomial predictor. Models were compared using Akaike Information Criterion (AIC; Akaike, 1974) and the Bayesian Information Criterion (BIC; Schwarz, 1978) values. Lower AIC and BIC values indicate a better model fit. Following identification of the best fitting developmental model, a random slope for age was added to examine whether there were significant individual differences in the development of neural risk processing. All models showed significant improvement with the addition of a random slope ($p < .001$). We also examined sex differences in the development of neural risk processing by adding sex as a main effect and interaction effect to the best fitting polynomial age model. Each adolescent's sex was dummy-coded with males as 0 and females as 1. Finally, given the influence that puberty has on brain development (Blakemore, Burnett, & Dahl, 2010), follow-up analyses included time-varying levels of pubertal development in the best fitting developmental model to evaluate the independent contribution of age on neural risk processing development.

Our second goal was to examine how peer attachment across ages 13 – 17 years was associated with the development of neural risk processing in the insula and

dACC. We first fitted a model that included sex and the best fitting age model (e.g., linear, quadratic or cubic) of insula or dACC risk processing. We then tested for main effects of peer attachment. Next, we fitted a model assessing associations over time (peer attachment X age), a model assessing sex differences (peer attachment X sex) and a model that included both two-way interactions. Finally, to rule out higher-order associations we also fitted a model with the three-way interaction among peer attachment, age, and sex (peer attachment X age X sex). Model fit was assessed by the evaluation of AIC. BIC values are reported for completeness but are not used in model selection as BIC values may perform worse with complex models such as models including interactions (Vrieze, 2012). Follow-up analyses included time-varying levels of parental attachment and pubertal development, to evaluate the independent contribution of peer attachment on neural risk processing over and above perceived parental attachment and pubertal development. Given that our models assessing sex-specific effects were exploratory, the results of these analyses are reported at a significance level of $p < .05$ (Bender & Lange, 2001).

Intra-class correlation coefficient (ICC). Mixed model analyses require that observations of longitudinal data are sufficiently nested in individuals and can be assessed with an intra-class correlation coefficient (ICC). ICC values were assessed using two-way mixed effects models with absolute agreement in SPSS, version 25. All ICC values of our study variables are above .10 indicating satisfactory nesting of data within individuals (see Table 4.1) (Cicchetti & Sparrow, 1981).

Results

Descriptive statistics

Descriptive statistics are shown in Table 4.1. Females scored higher on perceived peer attachment on T1 but did not differ from males on T2 – T4. Results of the whole-brain analysis are presented in Supplementary Tables S4.4 – S4.7 and correlations between study variables are shown in Supplementary Table S4.2. For descriptive purposes, developmental changes of peer attachment, behavioral performances on the lottery choice task (i.e., risk-preference) and the covariates of pubertal status and parental attachment were assessed using mixed model analyses (see Supplementary Tables S4.8-S4.9). The development of peer attachment differed between males and females ($B_{sex*\ age}$ = -0.09, SE = 0.03, p = .002). The level of peer attachment was stable for females ($B_{age(linear)}$ = -0.02, SE = 0.02, p = .511), whereas males started at a lower level (see Table 4.1) but increased ($B_{age\ (linear)}$ = 0.07, SE = 0.02, $p < .001$) in their perceived peer attachment to levels similar to females by age 17 years. No significant sex differences were found in the patterns of development of

behavioral risk-preference. Rather, risk-preference on the lottery choice task showed a linear decrease with age for both males and females ($B_{age\ (linear)}$ = -0.12, SE = 0.03, p < .001). Pubertal development increased with age and stabilized at age 17 ($B_{age\ (linear)}$ = 0.19, SE = 0.01, p < .001; $B_{age\ (quadratic)}$ = -0.03, SE = 0.01, p < .001) with higher levels of pubertal development for females than males across ages 13 – 17 years (B_{sex} = 0.64, SE = 0.04, p < .001). Finally, the level of parental attachment was stable over time ($B_{age\ (linear)}$ = -0.01, SE = 0.02, p = .644) and did not differ between males and females.

Development of neural risk processing

AIC and BIC values for the mixed models examining the development of insula and dACC risk processing are listed in Table 4.2. Results showed that the development of insula and dACC risk processing across ages 13 – 17 years was best described by a linear pattern.

As shown in Table 4.3, insula and dACC risk processing increased linearly across the measured period (right insula: B_{age} = 0.18, SE = 0.03, p < .001; left insula: B_{age} = 0.15, SE = 0.02, p < .001; and dACC: B_{age} = 0.18, SE = 0.03, p < .001). No main effect or interaction with sex was found in the development of insula and dACC risk processing. Controlling for time-varying levels of pubertal development did not change these results (see Supplementary Table S4.10).

Associations of peer attachment with neural risk processing

Linear mixed models were fitted to examine the association between peer attachment and neural risk processing across age and sex. AIC and BIC values are shown in Table 4.4. For the right insula, adding peer attachment as a predictor to our developmental model did not improve model fit. Moreover, allowing the association between peer attachment and risk processing to vary over time (peer attachment X age) did not improve model fit. However, including the interaction between peer attachment and sex improved model fit. To examine sex-specific changes over time in this association, we also assessed a model including the three-way interaction between peer attachment, sex, and age (peer attachment X sex X age). This model did not improve the model fit relative to the model including the interaction between peer attachment and sex, suggesting that the strength of two-way interaction between peer attachment and sex did not significantly change from ages 13 to 17 years. Therefore, for the right insula, the model including the two-way interaction between peer attachment and sex was selected as the best-fitting model. For the left insula and dACC, including peer attachment or higher-order interactions did not improve model fit. Final model parameters of the models including the interaction between peer attachment and sex are shown in Table 4.5.

Table 4.1. Means and standard deviations of peer attachment, behavioral and neural correlates of risk processing, and control variables

	T1				T2				T3				T4				ICC (95% CI)
	Male		Female		Male		Female		Male		Female		Male		Female		
	M	*SD*	*M*	*SD*	*M*	*SD*	*M*	*SD*	*M*	*SD*	*M*	*SD*	*M*	*SD*	*M*	*SD*	
Age	14.19	0.52	14.06	0.55	15.13	0.52	14.98	0.57	16.15	0.54	16.01	0.57	17.08	0.53	16.91	0.56	-
Peer attachment	**3.88**	**0.51**	**4.12**	**0.59**	3.99	0.45	4.14	0.58	4.08	0.45	4.14	0.50	4.11	0.41	4.07	0.67	.73 (.65 - .79)
Risk-preference	0.72	0.49	0.88	0.93	0.54	0.48	0.66	0.87	0.59	0.91	0.42	0.39	0.37	0.33	0.45	0.90	.46 (.31 - .58)
Right insula	0.03	0.05	0.03	0.05	0.46	0.67	0.47	0.58	0.75	1.04	0.54	0.74	0.61	1.09	0.61	0.77	.52 (.37 - .63)
Left insula	0.03	0.05	0.04	0.05	0.41	0.68	0.38	0.52	0.60	0.99	0.42	0.78	0.53	1.15	0.56	0.74	.46 (.32 - .58)
dACC	0.04	0.05	0.03	0.04	0.44	0.75	0.39	0.54	0.73	1.05	0.57	0.87	0.55	1.04	0.68	0.94	.49 (.35- .61)
Control variables																	
PD	**2.62**	**0.51**	**3.24**	**0.44**	**2.83**	**0.38**	**3.45**	**0.44**	**2.99**	**0.36**	**3.67**	**0.31**	**3.19**	**0.40**	**3.82**	**0.33**	.81 (.64 - .88)
Parental attachment	**4.10**	**0.48**	**4.25**	**0.48**	4.02	0.56	4.16	0.58	4.13	0.50	4.10	0.61	4.08	0.53	4.14	0.59	.86 (.82 - .89)

Note. Bold entries indicate significant differences between males and females at $p < .05$. T1-4 = time point 1 – 4; ICC = intra-class correlation coefficient; CI = confidence interval; dACC = dorsal anterior cingulate cortex; PD = pubertal development.

Table 4.2. AIC and BIC values for the developmental models of neural risk processing across ages 13 – 17 years

	Right insula		Left insula		dACC	
	AIC	BIC	AIC	BIC	AIC	BIC
Age						
Null	1402	1424	1420	1443	1482	1504
Linear	**1359**	**1386**	**1388**	**1415**	**1441**	**1468**
Quadratic	1357	1389	1386	1417	1439	1471
Cubic	1359	1395	1386	1422	1440	1476
Test for sex differences						
Age + sex	1361	1392	1390	1421	1443	1474
Age X sex	1363	1399	1392	1428	1444	1480

Note. Best fitting models are marked in bold. Sex differences in the development were assessed using the best fitting age models. For all three outcomes, the linear age model was the best fitting age model. AIC = Akaike Information Criterion; BIC = Bayesian Information Criterion; dACC = dorsal anterior cingulate cortex.

For right insula risk processing, we found a significant interaction between peer attachment and sex ($B_{attachment*sex}$ = -0.21, *SE* = 0.10, *p* = .034; see Figure 4.3). We performed simple slope analysis of this significant interaction to probe the direction of effect under the moderator variable (i.e., sex) (Holmbeck, 2002). In other words, we examined the magnitude and direction of the association between right insula risk processing and peer attachment separately for females and males. This simple slope analysis showed a significant positive association between peer attachment and neural risk processing only for males ($B_{attachment}$ = 0.19, *SE* = 0.09, *p* = .039); there was no significant association between peer attachment and right insula processing for females ($B_{attachment}$ = -0.03, *SE* = 0.06, *p* = .659).

Our results remained significant after controlling for time-varying levels of pubertal development and parental attachment (see Supplementary Table S4.11). As can be seen in Table 4.5, there was no significant main effect or interaction with peer attachment for the left insula and dACC. Results thus showed that for male adolescents the level of peer attachment was associated with *neural* risk processing (particularly in right insula) and the strength of this association was stable from ages 13 – 17 years.

As a supplemental analysis, we also assessed associations between peer attachment and *behavioral* performances on the task (i.e., risk-preference). No significant main effect of peer attachment or interaction effect with sex was found (see Supplementary Table S4.12).

Table 4.3. Parameter estimates (regression coefficient [*b*], standard error [*SE*] and significance level [*p*]) for the best fitting developmental model of neural risk processing across ages 13 – 17 years

	Right insula			Left insula			dACC		
	b	***SE***	***p***	***b***	***SE***	***P***	***b***	***SE***	***p***
Intercept	0.44	0.04	<.001	0.38	0.04	<.001	0.45	0.04	<.001
Age (linear)	0.18	0.03	<.001	0.15	0.03	<.001	0.18	0.02	<.001

Note. All models include a random slope for age. dACC = dorsal anterior cingulate cortex.

Table 4.4. AIC and BIC values of the models assessing associations of Peer attachment with neural risk processing and risk-preference

Model	Age + Sex		Age + Sex + peer attachment		Peer attachment X Age		Peer attachment X Sex		Peer attachment X Age + Peer attachment X Sex		Peer attachment X Age X Sex	
	AIC	**BIC**	**AIC**	**BIC**	**AIC**	**BIC**	**AIC**	**BIC**	**AIC**	**BIC**	**AIC**	**BIC**
Right insula	1360	1386	1361	1392	1361	1397	1359	1399	1363	1404	1363	1417
Left insula	1388	1415	1390	1421	1391	1427	1392	1433	1393	1434	1397	1452
dACC	1441	1468	1443	1474	1444	1480	1444	1484	1445	1486	1449	1503
Risk-preference	1423	1459	1425	1466	1427	1472	1427	1477	1427	1477	1427	1491

Note. Preferred models are marked in bold. AIC = Akaike Information Criterion, BIC = Bayesian Information Criterion.

Table 4.5. Parameter estimates (regression coefficient [*b*], standard error [*SE*] and significance level [*p*]) for the best fitting model on the association between peer attachment and neural risk processing moderated by sex

	Right insula			Left insula			dACC		
	b	***SE***	***p***	***b***	***SE***	***p***	***b***	***SE***	***p***
Intercept	0.47	0.05	<.001	0.41	0.05	<.001	0.47	0.05	<.001
Age (linear)	0.17	0.03	<.001	0.15	0.03	<.001	0.18	0.03	<.001
Sex	-0.06	0.08	.376	-0.05	0.07	.217	0.14	0.07	.463
Peer attachment	0.19	0.06	.015	0.09	0.08	.526	-0.05	0.08	.108
Peer attachment X Sex	-0.22	0.10	.034	-0.13	0.11	.232	-0.14	0.11	.196

Note. All models include a random slope for age. Male is coded as 0, female as 1. dACC = dorsal anterior cingulate cortex.

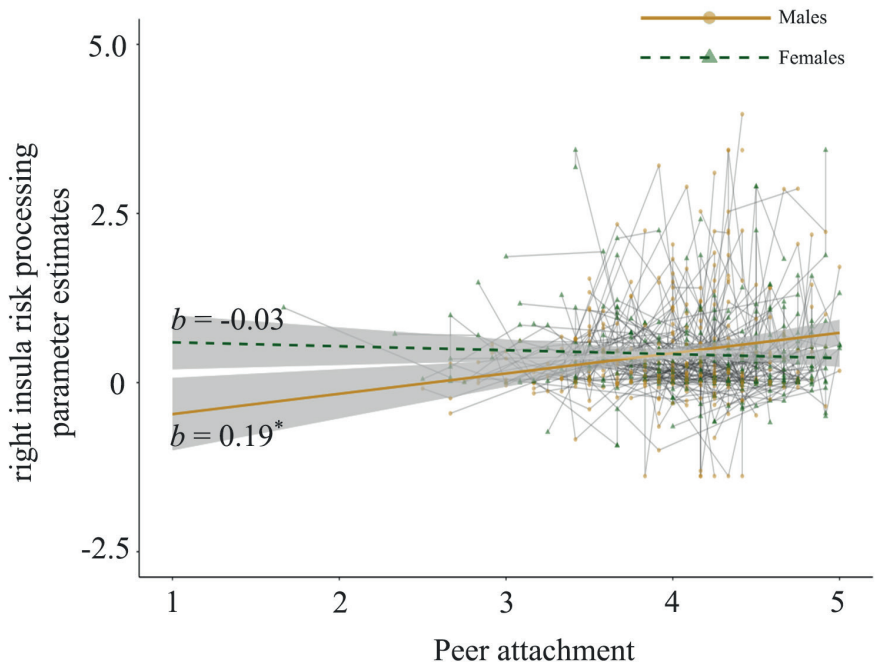

Figure 4.3. Associations between peer attachment and neural risk processing for males and females in the right insula. Shades around the regression lines represent the 95% confidence interval. * $p < .05$.

Discussion

The aims of this longitudinal study were to examine the development of neural risk processing across adolescence and to examine its associations with peer attachment. Results showed that the insula and dACC were consistently activated during neural risk processing across adolescence and showed a linear increase from ages 13 to 17 years. Furthermore, there was a positive association between peer attachment and right insula risk processing for male adolescents, and the strength of this association was stable across ages 13 – 17 years. The association between peer attachment and neural risk processing was not significant for female adolescents.

The current results present the first insight into the development of insula and dACC risk processing as well as providing evidence of longitudinal associations between peer attachment and right insula risk processing, particularly for male adolescents. With respect to our finding on the development, specifically linear increases in insula and dACC risk processing across ages 13 – 17 years, this finding is in line with previous cross-sectional studies that compared different age groups and demonstrated

higher activation during adolescence compared to childhood (Paulsen et al., 2012; van Duijvenvoorde et al., 2015). Specifically, Paulsen and colleagues (2012) reported linear age-related increases in insula and dACC activation during risk processing when comparing children, adolescents, and adults; whereas van Duijvenvoorde and colleagues (2015) reported heightened insula and dorsal medial prefrontal cortex activation in late adolescents compared to children and adults. Our finding clarifies the developmental pattern of insula and dACC activation during risk processing by examining within-person changes across adolescence. The found increase also concurs with the theory that the prefrontal cortex matures gradually during adolescence and gains control over adolescent risk-taking decision making (Casey et al., 2008; Steinberg, 2007). However, we note that some previous cross-sectional studies showed *lower* dACC activation during risk taking in adults compared to adolescents and children (van Leijenhorst et al., 2006; van Leijenhorst et al., 2010). These studies have either used tasks involving one risky gamble per trial or tasks in which the participant was asked to decide between a certain amount or a risky gamble (e.g., van Leijenhorst et al., 2006; van Leijenhorst et al., 2010). Whereas, in the current study, both high- and low-risk gambles were presented simultaneously to simulate decision options in the real world. That is, in real-world risky situations, individuals are often faced with two options, in which one option is relatively riskier than the other. Accordingly, both options have potential consequences that are often judged relative to one another. This paired presentation may have potentially increased the salience of high-risk choices.

Besides the neural development of risk processing, our finding of an association between higher peer attachment and greater neural risk processing in the right insula across ages 13 – 17 years, albeit only among males, is also noteworthy. Previous work showed that high peer attachment buffered the effect of peer conflict on the socio-emotional system (e.g., striatum and medial prefrontal cortex) during risk taking (Telzer et al., 2015), suggesting the protective effect of peer attachment against the negative effect of peer conflict on reward sensitivity. Prior neuroimaging studies focusing on risk sensitivity have demonstrated a crucial involvement of the *right* insula in decision risk—i.e., risk processing during or before choices (Mohr et al., 2010; van Duijvenvoorde et al., 2015) and risk-averse behavior (Van Duijvenvoorde et al., 2015). Our finding of higher right insula activation for adolescents high on peer attachment possibly indicates that the insula was effectively working to lead decision makers to exhibit caution and thoroughly evaluate risky options. The current study extends prior work by providing evidence that higher peer attachment is associated with increased neural processing of risk information. The findings seem to suggest the beneficial nature of peer attachment on brain function—i.e., prompting adolescents away from (rather than towards) risky choices.

Importantly though, the significant association between peer attachment and right insula processing was only found among *male* adolescents. Most previous studies that examined peer influences on adolescent brain functioning were based on relatively small samples and did not test sex differences in these associations. Our result on male-specific activation is not in line with the study by Braams and colleagues (2014) who explored sex differences. That study found a positive association between friendship quality and ventral striatum activation when winning a gamble for a friend for females, but not males (Braams et al., 2014). Differences between the current study and the prior study may be explained by differences in measured neural processes – e.g., risk processing versus reward processing (d'Acremont & Bossaerts, 2008; van Duijvenvoorde et al., 2015) as well as existing sex differences in the nature of attachment to peers. That is, female adolescents value peer intimacy more and seek peer support more, whereas male adolescents prefer spending time with their peers based on common interests (Gorrese & Ruggieri, 2012; Rose & Rudolph, 2006). Thus, winning money for a friend on a gamble may be perceived as more rewarding for females (Braams et al., 2014) due to the value they place on their peer network as a secure base. In contrast, risk-taking behavior may be a way to gain recognition from peers and be part of a peer group particularly for male adolescents (Michael & Ben-Zur, 2007; Piko, 2000). Indeed, a prior study showed that social exclusion by peers increased levels of risk taking particularly for adolescents who were more susceptible to peer influences, and this was negatively related to activation in the lateral prefrontal cortex, a region important for exerting behavioral control (Eshel et al., 2007; Peake, Dishion, Stormshak, Moore, & Pfeifer, 2013). Thus, male adolescents who felt greater psychological security provided by peers exhibited more careful brain processing when evaluating risky options, whereas adolescents lacking good quality relationships may be more likely to take risks as a part of their efforts to overcome negative feelings resulting from their low acceptance by peers (Brady, Dolcini, Harper, & Pollack, 2009).

Our data revealed that the effect of peer attachment was only observed for risk-related neural processing, but not for the behavioral measure of risky decision-making (i.e., risk preference). The reason for the association of peer attachment with neural and not behavioral measures may be due to the fact that peer attachment is related to the processing of risk, which is captured by the neural activation, rather than the outcome, which is reflected through behavioral choices. That is, adolescents evaluated risk information related to options *before* making a choice. Moreover, laboratory tasks may be limited in capturing real-world behavioral responses, but risk-related neural processing may be able to more accurately represent individual differences in neurobiological processes (Richards, Plate, & Ernst, 2013). In addition, although we were not able to test this, we note that associations between neural

risk processing and peer attachment may differ depending on the nature of the peer interactions. That is, adolescents tend to select and associate with similarly behaving peers, and peer socialization through deviant peer association is known to be one of the strongest predictors of adolescent delinquent behaviors (Dishion & Owen, 2002; Dishion & Patterson, 2016). Indeed, prior studies showed that interacting with a risk-promoting peer was related to higher risk-taking behaviors, whereas interacting with a cautious peer was associated with lower risk-taking behaviors (see Dishion & Patterson, 2016 for review). Moreover, a recent study reported a longitudinal association between adolescents' affiliation with substance using peers and lowered insula activation during risk processing (Kim-Spoon et al., 2019). As such, future studies are needed to investigate how the nature of peer attachment (e.g., deviant or low-risk peers) may relate to adolescents' neural risk processing.

An important strength of this study is the inclusion of adolescents from an Appalachian region of southwestern Virginia. This region is a distinct geographic and cultural area of the United States and adolescents from these regions are often from low household incomes (Census, 2017). Moreover, adolescents from these rural regions show relatively higher incidences of health risk behaviors such as substance use or risky sexual behavior (Moreland, Raup-Krieger, Hecht, & Miller-Day, 2013; Wewers, Katz, Fickle, & Paskett, 2006), providing implications for preventive intervention efforts. Another methodological strength is that peer attachment was associated with neural risk processing even when controlling for parental attachment. This demonstrates that the level of attachment to peers uniquely contributes to neural risk processing across adolescence rather than being attached to people (e.g., peers and parents) in general.

Despite its strengths, some limitations of this study must be noted. First, more research is necessary to determine the generalizability of our findings and possible variations to these findings due to different cultural contexts. Second, in the current study risk processing was defined as the variance in potential outcomes, and the lottery choice task did not include gambles where potential losses were possible. Although the absence of a high rewarding gain could be interpreted as a loss in our study, the current results may not be generalizable to all forms of risk taking, as some forms of risk-taking behavior in everyday life include potential harmful outcomes (Schonberg et al., 2011). Third, the associations between peer attachment and neural risk processing were correlational, so causal effects could not be inferred. Lastly, our analyses on sex differences were exploratory. Future research utilizing even larger samples is necessary to replicate our findings and gain a better understanding of how peer attachment may relate to neural risk processing for both male and female adolescents.

To our knowledge, this is the first prospective longitudinal study demonstrating how peer attachment is related to the development of brain functioning related to risk processing throughout adolescence. We observed that neural sensitivity to risk in the insula and dACC increased from ages 13 – 17 years and that individual differences in right insula risk processing was associated with levels of peer attachment, but only for males. The found increases in neural sensitivity for risk suggest that adolescents become more prudent decision makers across adolescence, according to the brain maturation that facilitates the consideration of the potential riskiness in their decisions. In addition, the found association between peer attachment and neural risk processing for males has important implications for preventive interventions as male adolescents have been shown to engage in higher levels of risk behaviors compared to female adolescents (Moffitt & Caspi, 2001). Also, lower neural sensitivity toward risk has been shown to predict later health-risk behaviors such as substance abuse (Kim-Spoon et al., 2019). Present findings demonstrate the potential role of peer relationships in adolescent risk taking, suggesting that greater risk sensitivity in the male adolescent brain may be a mechanism by which supportive peer relationships could demote risky behaviors during adolescence.

Supplementary material

Risk-preference parameter

We computed a risk-preference parameter (α) using a standard power utility function (Holt & Laury, 2002):

$$U(x) = x^{a} \tag{1}$$

where *U* is the utility of *x*, *x* is the amount of money that could be won, and α is the risk preference parameter, with α > 1 indicating risk-seeking preferences, α = 1 indicating risk neutrality, and α < 1 indicating risk aversion. *EU* (i.e., subjective value) for each gamble was computed:

$$EU = P * U_{unchosen} + P * U_{chosen.} \tag{2}$$

Each adolescent's set of choices in the task was fitted to a logistic function using maximum likelihood estimation:

$$P\,(chosen\,) = \frac{1}{1 + e^{\gamma(EUunchosen - EUchosen)}} \tag{3}$$

where *P* (*chosen*) represents the predicted probability of the chosen gamble, γ represents the inverse temperature which is a measure for consistency in choices of participants.

Coefficient of Variation (CV)

The magnitude of risk on each gamble was quantified by computing the coefficient of variation (CV). The CV is a scale-free metric and is computed by dividing the standard deviation of the potential outcomes of a gamble by the expected value (EV) of that gamble. The EV is a measure of average expected outcome of a gamble and is defined as:

$$EV = P_{high} * V_{high} + P_{low} * V_{low} \tag{4}$$

CV is defined as:

$$CV = \frac{\sqrt{P_{high}\,(V_{high} - EV)^2 + P_{low}\,(V_{low} - EV)^2}}{EV} \tag{5}$$

where P_{high} and P_{low} represent the probability of respectively the high and low outcome gamble and V_{high} and V_{low} represent respectively the high and low monetary outcome. Previous studies have shown that the CV is a stronger predictor for explaining choice behavior compared to other economic measures of risk (i.e., standard deviation or variance) because outcomes are coded by the relative risk as opposed to the absolute outcome (Bach, Symmonds, Barnes, & Dolan, 2017; Weber, Shafir, & Blais, 2004). Higher values of CV corresponding to higher risk options (see Supplementary Table S4.1).

Mixed model analyses

We fitted our models according to the modeling approach suggested by Braams, van Duijvenvoorde, Peper, and Crone (2015). The formal notation of a linear age model is:

Level 1

$$Y_{ti} = \pi_{oi} + \pi_{1i} * (Age\ Linear)_{ti} + e_{ti}$$

Level 2

$$\pi_{0i} = Y_{00} + r_{oi}$$

$$\pi_{1i} = Y_{10} + r_{1i}$$

Where Y_{ti} represents the level of neural risk processing at the *t'th* time point for the *i'th* individual. On the second level π_{oi} includes the fixed (Y_{00}) and random (r_{0i}) intercept and π_{1i} include the fixed (Y_{10}) and random (r_{0i}) slope. *E* represents the non-modeled within-person variance. The R code of the models is:

model <- lme (neural risk processing ~ poly(age,1) + predictors + control variables, random = ~1|subject, data = datafile name, method = "ML")

The model can be expanded in a polynomial way by replacing poly(age,1) with poly(age,2) to fit a quadratic model and with poly(age,3) to fit a cubic model. By replacing ~1|subject with ~age|subject one can fit a random slope for age.

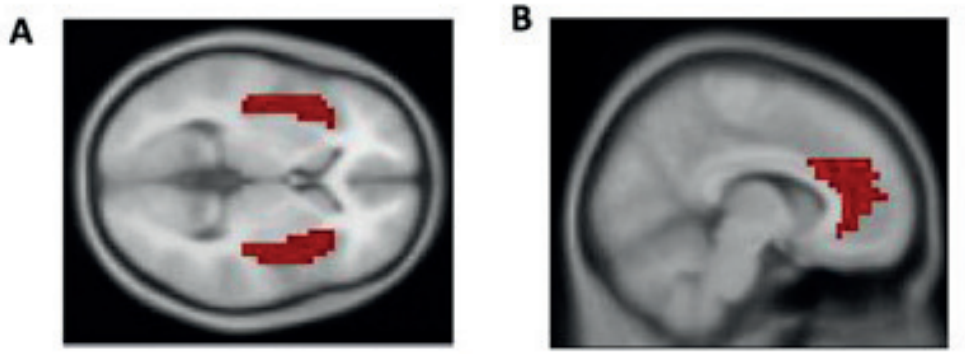

Supplementary Figure S4.1. A) Image depicting the bilateral insular cortex and B) dorsal anterior cingulate cortex (dACC) regions of interest as anatomically defined by the Automated Anatomical Labeling (AAL) atlas for functional neuroimaging data (Tzourio-Mazoyer et al., 2012).

Supplementary Table S4.1. Gamble information on the lottery choice task

Low-Risk Option						High-Risk Option					
Low Outcome	High Outcome	Pr. Low Outcome	Pr. High Outcome	EV	CV	Low Outcome	High Outcome	Pr. Low Outcome	Pr. High Outcome	EV	CV
$1.60	$2.00	80%	20%	1.68	0.09	$0.10	$3.85	80%	20%	0.85	1.76
$1.60	$2.00	70%	30%	1.72	0.10	$0.10	$3.85	70%	30%	1.23	1.40
$1.60	$2.00	60%	40%	1.76	0.11	$0.10	$3.85	60%	40%	1.60	1.15
$1.60	$2.00	50%	50%	1.80	0.11	$0.10	$3.85	50%	50%	1.98	0.95
$1.60	$2.00	40%	60%	1.84	0.10	$0.10	$3.85	40%	60%	2.35	0.78
$1.60	$2.00	30%	70%	1.88	0.09	$0.10	$3.85	30%	70%	2.73	0.63
$1.60	$2.00	20%	80%	1.92	0.08	$0.10	$3.85	20%	80%	3.10	0.48
$1.60	$2.00	10%	90%	1.96	0.06	$0.10	$3.85	10%	90%	3.48	0.32

Note. Pr. = probability; EV = expected value; CV = coefficient of variation.

Supplementary Table S4.2. Correlations among peer attachment, behavioral and neural correlates of risk processing

	1	2	3	4	5	6	7	8	9	10	11	12	13	14	15	16	17	18	19	20	21	22	23	24
1 Peer attachment T1	-																							
2 Peer attachment T2	**.52**	-																						
3 Peer attachment T3	**.43**	**.46**	-																					
4 Peer attachment T4	**.39**	**.29**	**.35**	-																				
5 Parent attachment T1	**.32**	**.27**	**.34**	**.20**	-																			
6 Parent attachment T2	**.24**	**.26**	**.29**	.12	**.65**	-																		
7 Parent attachment T3	.11	.15	**.32**	**.18**	**.58**	**.69**	-																	
8 Parent attachment T4	**.04**	**.08**	**.20**	**.19**	**.49**	**.53**	**.68**	-																
9 Risk-preference T1	.06	-.04	-.12	-.07	-.07	-.12	**-.15**	-.12	-															
10 Risk-preference T2	.02	.05	**-.16**	.05	-.14	**-.18**	**-.22**	-.13	**.28**	-														
11 Risk-preference T3	.07	.01	-.02	.02	-.06	-.13	-.11	-.14	**.39**	**.18**	-													
12 Risk-preference T4	-.05	.02	-.02	-.09	.04	.02	.11	.07	.01	.11	.06	**-**												
13 dACC T1	.03	.01	.01	.09	-.05	**-.16**	**-.22**	**-.17**	**-.18**	-.06	-.04	-.05	-											
14 dACC T2	-.07	-.04	-.01	.00	-.03	.04	-.03	.02	-.08	**-.16**	-.12	-.09	**.12**	-										
15 dACC T3	-.09	-.08	-.08	-.08	.04	**.16**	.11	.05	-.10	**-.20**	-.14	-.12	.11	**.19**	-									
16 dACC T4	.01	.05	.13	-.12	-.02	-.06	-.12	**-.18**	.10	**-.21**	-.07	**-.23**	**.21**	**.24**	**.33**	-								
17 Left insula T1	-.01	.05	-.04	**.18**	-.05	-.02	.01	-.06	**-.29**	.06	-.04	-.06	**.45**	.10	.15	.09	-							
18 Left insula T2	**-.18**	-.02	.01	-.06	-.12	-.04	-.05	-.02	-.09	**-.16**	-.10	-.13	**.16**	**.75**	.08	**.26**	.13	-						
19 Left insula T3	.01	-.03	-.09	.08	-.09	-.02	.01	-.03	-.10	-.14	-.09	-.09	**.18**	**.19**	**.67**	**.22**	**.17**	.15	-					
20 Left insula T4	.09	.13	**.18**	.03	.02	-.09	-.08	**-.17**	.07	**-.18**	-.09	**-.21**	**.20**	**.16**	**.20**	**.78**	.07	**.26**	**.31**	-				
21 Right insula T1	.05	.08	.04	**.19**	.08	.02	.02	-.01	**-.23**	-.11	-.06	-.12	**.47**	**.17**	.14	**.24**	**.65**	**.18**	**.16**	**.24**	-			
22 Right insula T2	-.11	.02	.07	-.07	-.09	-.02	**-.05**	.01	-.09	-.10	-.11	-.13	.14	**.77**	.11	**.28**	.12	**.86**	.09	**.26**	**.18**	-		
23 Right insula T3	.01	-.03	-.06	.04	-.05	.03	**.03**	.01	-.11	**-.16**	.06	-.08	**.16**	**.20**	**.73**	**.21**	**.19**	.12	**.85**	**.25**	**.16**	.09	-	
24 Right insula T4	.05	.08	.10	-.04	-.10	-.13	**-.11**	-.13	.13	**-.21**	-.04	**-.19**	.14	**.22**	**.26**	**.78**	.04	**.28**	**.35**	**.82**	.14	**.26**	**.31**	-

Note. Bold entries are correlation coefficient significant at $p < .05$ (uncorrected). T1 – 4 = time point 1 – 4.

Supplementary Table S4.3. Number of scans obtained at T1, T2, T3, and T4

Time- point	Number of participants	Valid scans	Scans excluded		
			Excessive motion (> 3 mm)	MRI contraindications[†]	Other [‡]
T1	157	141	10	3	3
T2	150	136	1	10	3
T3	143	126	0	7	10
T4	142	129	0	9	4

Note. [†] dental braces, claustrophobia, or recent work with metals; [‡] technical problems or artifacts.

Supplementary Table S4.4. Parametric regressor of coefficient of variation for chosen options during the decision phase at Time 1

Cluster #	Region	Side	k	*T*	MNI Coordinates		
					x	*y*	*z*
1	Insular Cortex	R	605	8.24	30	20	-11
	Insular Cortex	R		7.27	45	17	-2
2	Anterior Cingulate Cortex	R	1798	8.14	3	35	22
	Anterior Cingulate Cortex	R		6.25	6	41	4
	Pallidum	R		5.91	12	2	-5
3	Insular Cortex	L	430	7.79	-30	17	-14
	Insular Cortex	L		7.65	-39	17	-5
4	Middle Cingulate Cortex	R	111	4.84	3	-16	34
5	Middle Occipital Lobe	L	93	4.14	-36	-94	1
	Middle Occipital Lobe	L		4.08	-27	-97	-8
6	Middle Occipital Lobe	R	45	4.09	24	-100	1
	Inferior Occipital Gyrus	R		3.59	36	-88	-8
7	Precentral Gryus	R	8	3.54	42	5	31
8	Superior Orbitofrontal Cortex	R	5	3.43	21	56	-8

Note. Side = left/ right hemisphere, k = number of voxels in cluster, T = t-value reported at $p_{FWE} < .05$, at a primary uncorrected threshold of $p < .001$, MNI = Montreal Neurological Institute. All activations reported here survive whole-brain family-wise error multiple comparisons correction at a threshold of $p < .05$, with an initial uncorrected threshold of $p < .001$.

Supplementary Table S4.5. Parametric regressor of coefficient of variation for chosen options during the decision phase at Time 2

					MNI Coordinates		
Cluster #	**Region**	**Side**	**k**	***T***	***x***	***y***	***z***
1	Anterior Cingulate Cortex	R	2960	8.10	6	38	22
	Insular Cortex	R		8.04	30	20	-11
	Pallidum	R		7.30	12	5	-2
2	Inferior Frontal Gyrus	L	418	7.85	-36	23	-5
	Insular Cortex	L		7.51	-33	20	-11
	Inferior Frontal Gyrus	L		4.19	-42	14	10
3	Middle Occipital Lobe	R	569	6.60	33	-91	1
	Middle Occipital Lobe	R		6.56	21	-100	1
	Inferior Occipital Lobe	R		6.53	27	-94	-5
4	Middle Occipital Lobe	L	527	5.90	-33	-91	1
	Inferior Occipital Lobe	L		5.68	-21	-97	-5
5	Precentral Gyrus	L	29	5.15	-51	-1	49
6	Precentral Gyrus	R	159	4.46	45	2	46
	Precentral Gyrus	R		4.30	48	5	34
7	Middle Occipital Gyrus	L	60	4.30	-24	-73	31
	Superior Occipital Gyrus	L		4.17	-18	-67	37
8	Vermis		30	4.21	0	-52	-29
9	Middle Frontal Gyrus	R	62	4.20	30	56	28
	Middle Frontal Gyrus	R		3.75	21	50	25
10	Superior Parietal Lobe	R	41	4.05	33	-55	58
11	Superior Occipital Lobe	R	39	4.00	27	-64	40
	Precuneus	R		3.58	12	-70	40
	Middle Occipital Lobe	R		3.53	33	-70	31
12	Middle Frontal Gyrus	R	20	3.99	42	53	13
13	Inferior Parietal Lobe	L	26	3.97	-27	-55	52
15	Cerebellum	L	12	3.80	-33	-58	-26
16	Superior Frontal Gyrus (orbital)	L	6	3.61	21	44	-14
17	Superior Frontal Gyrus (orbital)	R	7	3.50	21	56	-11

Note. Side = left/ right hemisphere, k = number of voxels in cluster, T = t-value reported at $p_{FWE} < .05$, at a primary uncorrected threshold of $p < .001$, MNI = Montreal Neurological Institute. All activations reported here survive whole-brain family-wise error multiple comparisons correction at a threshold of $p < .05$, with an initial uncorrected threshold of $p < .001$.

Supplementary Table S4.6. Parametric regressor of coefficient of variation for chosen options during the decision phase at Time 3

					MNI Coordinates		
Cluster #	**Region**	**Side**	**k**	***T***	***x***	***y***	***z***
1	Anterior Cingulate Cortex	R	3957	8.29	6	38	22
	Insular Cortex	R		7.95	27	23	-8
	Insular Cortex	L		7.77	-33	14	-11
	Insular Cortex	R		7.07	36	17	-11
2	Medial Orbitofrontal Cortex	R	151	5.57	24	47	-14
3	Angular Gyrus	R	131	5.15	33	-64	40
4	Cerebellum	L	124	4.83	-33	-61	-26

Note. Side = left/ right hemisphere, k = number of voxels in cluster, T = t-value reported at $p_{FWE} < .05$, at a primary uncorrected threshold of $p < .001$, MNI = Montreal Neurological Institute. All activations reported here survive whole-brain family-wise error multiple comparisons correction at a threshold of $p < .05$, with an initial uncorrected threshold of $p < .001$.

Supplementary Table S4.7. Parametric regressor of coefficient of variation for chosen options during the decision phase at Time 4

					MNI Coordinates		
Cluster #	**Region**	**Side**	**k**	***T***	***x***	***y***	***z***
1	Insular Cortex	R	3636	8.55	36	20	-11
	Middle Cingulate Cortex	R		8.35	6	-16	31
	Anterior Cingulate Cortex	R		8.17	6	35	34
	Insular Cortex	R		7.67	33	26	-5
	Insular Cortex	L		7.12	-36	23	-2
2	Middle Occipital Gyrus	R	3914	7.63	24	-91	1
	Middle Occipital Gyrus	L		6.47	-30	-91	-2
	Middle Occipital Gyrus	R		5.79	33	-88	7
3	Middle Frontal Gyrus	R	59	5.27	36	44	4

Note. Side = left/ right hemisphere; k = number of voxels in cluster; T = t-value reported at $p_{FWE} < .05$, at a primary uncorrected threshold of $p < .001$; MNI = Montreal Neurological Institute. All activations reported here survive whole-brain family-wise error multiple comparisons correction at a threshold of $p < .05$, with an initial uncorrected threshold of $p < .001$.

Supplementary Table S4.8. AIC and BIC values for the models describing the development of peer attachment, pubertal development, parental attachment, and risk-preference across ages 13 – 17 years

	Peer attachment		Pubertal development		Parental attachment		Risk preference	
	AIC	**BIC**	**AIC**	**BIC**	**AIC**	**BIC**	**AIC**	**BIC**
Age								
Null	912	939	794	816	789	816	1440	1467
Linear	911	943	646	673	791	822	1423	1454
Quadratic	911	947	636	668	789	825	1424	1460
Cubic	913	954	638	674	790	831	1426	1467
Test for sex differences†								
Age + sex	912	948	496	532	787	828	1425	1461
Age X sex	905	946	498	543	789	838	1425	1465

Note. Best fitting models are marked in bold. AIC = Akaike Information Criterion, BIC = Bayesian Information Criterion. †Sex differences in the development were assessed using the best fitting age models. The model for peer attachment and risk-preference include a linear age term and no significant effects were found for higher-order age models (quadratic, cubic). The model for pubertal development includes a quadratic age term. Given that for parental attachment the null model was the best fitting model we assessed potential sex effects with different age models (linear, quadratic, cubic) but no effects of sex were found.

Supplementary Table S4.9. Parameter estimates (regression coefficient [*b*], standard error [*SE*] and significance level [*p*]) for the best fitting developmental model of peer attachment, pubertal development, parental attachment and risk-preference across ages 13 – 17 years

	Peer attachment			Pubertal development			Parental attachment			Risk preference		
Fixed effects	***b***	***SE***	***p***	***b***	***SE***	***p***	***b***	***SE***	***p***	***b***	***SE***	***p***
Intercept	4.03	0.04	<.001	2.91	0.03	<.001	0.00	0.04	.975	0.58	0.03	<.001
Pubertal development	0.00	0.05	.997	-	-	-	-0.05	0.04	.226	0.01	0.06	.914
Age												
Linear	0.07	0.02	<.001	0.19	0.01	<.001	-0.01	0.02	.644	-0.12	0.03	<.001
Quadratic	-	-	-	-0.03	0.01	<.001	-	-	-	-	-	-
Sex	0.08	0.07	.157	0.64	0.04	<.001	-	-	-	-	-	-
Age x sex	-0.09	0.03	.002	-	-	-	-	-	-	-	-	-

Note. All models include random slopes for age. Males are coded as 0, females as 1.

Supplementary Table S4.10. Parameter estimates (regression coefficient [*b*], standard error [*SE*] and significance level [*p*]) for the best fitting developmental model of neural risk processing across ages 13 – 17 years controlled for pubertal development

	Right insula			Left insula			dACC		
	b	***SE***	***p***	***b***	***SE***	***p***	***b***	***SE***	***p***
Intercept	0.44	0.04	<.001	0.38	0.04	<.001	0.44	0.04	<.001
Pubertal development	-0.02	0.06	.719	-0.03	0.03	.634	-0.05	0.06	.372
Age (linear)	0.18	0.03	<.001	0.16	0.06	<.001	0.19	0.03	<.001

Note. All models include a random slope for age. dACC = dorsal anterior cingulate cortex.

Supplementary Table S4.11. Parameter estimates (regression coefficient [*b*], standard error [*SE*] and significance level [*p*]) for the best fitting model on the association between peer attachment and neural risk processing moderated by sex controlled for pubertal development and parental attachment

	Right insula			Left insula			dACC		
	b	***SE***	***p***	***b***	***SE***	***p***	***b***	***SE***	***p***
Intercept	0.45	0.05	<.001	0.40	0.05	<.001	0.46	0.06	<.001
Pubertal development	-0.01	0.07	.947	-0.02	0.07	.782	-0.05	0.07	.481
Parental attachment	-0.02	0.05	.755	-0.03	0.06	.590	0.01	0.06	.893
Age (linear)	0.17	0.03	<.001	0.15	0.03	<.001	0.19	0.03	<.001
Sex	-0.05	0.08	.499	-0.03	0.08	.730	-0.02	0.08	.826
Peer attachment	0.19	0.08	.014	0.11	0.08	.190	0.13	0.08	.118
Peer attachment X Sex	-0.22	0.10	.033	-0.13	0.11	.228	-0.14	0.11	.191

Note. All models include a random slope for age. Male is coded as 0, female as 1. dACC = dorsal anterior cingulate cortex.

Supplementary Table S4.12. Parameter estimates (regression coefficient [*b*], standard error [*SE*] and significance level [*p*]) for the best fitting model on the association between peer attachment and risk-preference moderated by sex

	Risk-preference		
	b	***SE***	***p***
Intercept	0.58	0.05	<.001
Pubertal development	-0.01	0.07	.938
Parental attachment	-0.07	0.06	.211
Age (linear)	-0.12	0.03	<.001
Sex	-0.01	0.08	.911
Peer attachment	-0.05	0.08	.531
Peer attachment X Sex	0.14	0.11	.190

Note. All models include a random slope for age. Male is coded as 0, female as 1.